Dyes and Pigments 88 (2010) 166–173

Contents lists available at ScienceDirect

Dyes and Pigments

journal homepage: www.elsevier.com/locate/dyepig

The synthesis of thermally-stable red dyes for LCD color filters and analysis of their aggregation and spectral properties

Chun Sakong [a], Young Do Kim [a], Jae-Hong Choi [b], Chun Yoon [c], Jae Pil Kim [a,*]

[a] Department of Materials Science and Engineering, Seoul National University, Seoul 151-744, Republic of Korea
[b] Department of Textile System Engineering, Kyungpook National University, 1370 Sankyuk-dong, Buk-gu, Daegu 702-701, Republic of Korea
[c] Department of Chemistry, Sejong University,98 Gunja-dong, Gwangjin-gu, Seoul 143-747, Republic of Korea

ARTICLE INFO

Article history:
Received 2 March 2010
Received in revised form
29 May 2010
Accepted 7 June 2010
Available online 16 June 2010

Keywords:
Color filters
Dye-based color filters
Thermal stability
Transmittance
Intermolecular interaction
Aggregation

ABSTRACT

Three thermally-stable red dyes of azo, quinacridone and perylene derivatives were synthesized and dye-based color filters were manufactured for use in liquid crystal displays. The aggregation behavior of the dyes and their spectral properties in film state were investigated using field emission scanning electron microscopy and concentration-dependent spectroscopy. Aggregate size was related to the geometry of the three dye types rather than their size, with average aggregate sizes ranging from 35 nm (azo), 80 nm (quinacridone) to 25 nm (perylene). Aggregation behavior affected the spectral property of the red color filter, resulting in weaker and broader transmittance spectrum with higher aggregation.

1. Introduction

Color filter is a key component of the thin-film transistor liquid crystal displays (TFT-LCDs) [1,2]. Conventional fabrication process of color filters is the pigment dispersion method where pigments are used as colorants [3]. Although this process is widely used in the flat panel displays industry, it has some disadvantages such as the complicated process, waste of photoresist and low chromaticity of the manufactured color filters [4].

Recently, pigment-based ink-jet printing method has been studied to simplify the complicated process and to reduce manufacturing cost of LCD color filters [5–8]. But, this method has the limitation of easy blocking of ink-jet nozzle by pigment particles used and color filters manufactured by this method also have low chromatic properties. In order to overcome these problems, ink-jet printing method where dyes are used for higher solubility and superior color saturation property has been proposed as an alternative. However, for dyes to be used for color filters, their lower thermal properties have to be overcome [9].

In our previous report [10], ink-jetted color filters with thermally-stable dyes were prepared and their characteristics were examined. The dyes had sufficient thermal stabilities for LCD color filters and the dye-based color filters had superior chromatic properties compared to those of pigment-based ones.

However, dyes generally have different aggregation behaviors according to their chemical species and these aggregation effects may change the spectral properties, such as transmittance and sharpness of color filters. The aggregation behavior of dye is greatly influenced by molecular geometry and intermolecular interaction. Therefore, to enhance the chromatic properties of dye-based color filters, especially transmittance, more understanding on the relationship between dye structures and their aggregation behaviors should be necessary.

In this study, we synthesized three thermally-stable red dyes of azo, quinacridone and perylene derivatives and the influence of dye structure both on their aggregation behaviors and spectral properties in the prepared color filters was studied. The change of dye aggregate size was investigated through the field emission scanning electron microscopy (FE-SEM). The transmittance of dye-based color filters was also measured to analyze the influence of aggregation behavior on the spectral characteristics.

* Corresponding author. Tel.: +82 2 880 7187; fax: +82 2 880 7238.
E-mail address: jaepil@snu.ac.kr (J.P. Kim).

0143-7208/$ – see front matter © 2010 Elsevier Ltd. All rights reserved.
doi:10.1016/j.dyepig.2010.06.003

2. Experimental

2.1. Materials and instrumentations

5-amino-1-naphthalene sulfonic acid and 5,12-dihydro-quino [2,3-b]acridone-7,14-dione purchased from TCI, 1-naphthol-3,6-disulfonic acid sodium salt, perylene-3,4,9,10-tetracarboxylic dianhydride, 4-chloroaniline, m-cresol, isoquinoline, fuming sulfuric acid (20%) and sulfuric acid (98%) from Sigma–Aldrich were used without purification further. All chemicals used in this study were of Synthesis-grade agent. Transparent glass substrate was provided from Paul Marienfeld GmbH & Co. KG. and hydrophilic acrylic binder of LGM 3050 was supplied by LG Micron Co., Ltd.

^{1}H NMR spectra were recorded by Bruker Avance 500 at 500 MHz using DMSO-d_6 as the solvent and TMS as the internal standard. Fourier transform infrared (FT-IR) spectra were recorded in the form of KBr pellets on a Perkin Elmer Spectrum 2000 FT-IR spectrometer. Matrix Assisted Laser Desorption/Ionization Time of Flight (MALDI-TOF) mass spectra were collected on a Voyager-DE STR Biospectrometry Workstation with a-cyano-4-hydroxycynamic acid (CHCA) as matrix. Absorption and transmittance spectra were measured with an HP 8452A spectrophotometer. Thermogravimetric analysis (TGA) was conducted under nitrogen at a heating rate of 10 °C min^{-1} with a TA Instruments Thermogravimetric Analyzer 2050.

2.2. Synthesis and characterizations

2.2.1. Synthesis of an azo dye (Dye 1) [11]

5-amino-1-naphthalene sulfonic acid 2.45 g (10 mmol) in 80 ml of water was dissolved by adding 10 ml of 7% potassium hydroxide aqueous solution. After cooling to 0–5 °C, 0.76 g (11 mmol) of sodium nitrite in 5 ml of water was added to the solution followed by the dropwise addition of 3 ml of 37% hydrochloric acid, maintaining the reaction temperature at 0–5 °C. After diazotization was complete (~2 h), the prepared diazonium salt liquor was added to 1-Naphthol-3,6-disulfonic acid sodium salt 5.8 g (10 mmol), dissolved in 70 ml of water at pH 5, maintaining the coupling solution at 0–5 °C and pH 4 and 5. The solution was stirred for 2 h and aq potassium chloride solution (3 mass %) was added to salt out the dye. The precipitate formed was filtered, washed with water and dried in a vacuum oven at 50 °C. The crude product was refluxed in ethanol for 2 h, hot filtered, washed with hot ethanol and subsequently dried in a vacuum oven at 50 °C. Purity of the dye was confirmed by thin layer chromatography using isopropanol/acetone/ammonium water (2:2:1) as the mobile phase. The yields, ^{1}H NMR, FT-IR and Mass data of the dye are given below.

Yield 85.5%;

^{1}H NMR (DMSO-d_6, ppm): 17.42 (s, 1H), 8.87 (d, 1H), 8.25 (d, 2H), 8.11 (d, 1H), 7.93 (s, 1H), 7.78 (d, 1H), 7.75 (t, 1H), 7.69 (s, 1H);

FT-IR (KBr, cm^{-1}): 1619 (C=O), 1233, 1069 (S=O), 625 (S–O);

MALDI-TOF MS: m/z 652.80 (100%, $[M + 2K]^+$).

2.2.2. Synthesis of a quinacridone dye (Dye 2) [12]

5,12-dihydro-quino[2,3-b]acridine-7,14-dione 1.56 g (5 mmol) was dissolved in 50 ml of sulfuric acid (98%) and the ensuing purple solution was heated at 110 °C for 14 h under a nitrogen atmosphere. The solution was cooled and poured into 300 ml of DMF, and slowly added to 2,000 ml of acetone to give a red precipitate which was filtered, washed with acetone and dried. The precipitate was dissolved in 300 ml of water and the solution was carefully neutralized using 7% aq potassium bicarbonate solution over 1 hr. After the addition of potassium chloride (100 g) to the solution, the precipitate formed was filtered, washed with ethanol and dried at 50 °C.

The crude product was dissolved in 3,000 ml of DMF, then the yellow–orange solution was filtered and the solvent was removed by rotary evaporation. The resulting dye was dried in a vacuum oven at 50 °C and its purity was confirmed by thin layer chromatography using isopropanol/acetone/ammonium water (2:2:1) as the mobile phase. The yields, ^{1}H NMR, FT-IR and Mass data of the dye are given below. Yield 73.6%;

^{1}H NMR (DMSO-d_6, ppm): 11.93 (s, 2H), 8.49 (s, 2H), 8.47 (s, 2H), 7.94 (d, 2H), 7.48 (d, 2H);

FT-IR (KBr, cm^{-1}): 3420 (N–H), 1619 (C=O), 1233, 1069 (S=O), 625 (S–O);

MALDI-TOF MS: m/z 548.63 (100%, $[M + 2K]^+$).

2.2.3. Synthesis of a perylene dye (Dye 3) [10,13]

A mixture of perylene-3,4,9,10-tetracarboxylic dianhydride 0.98 g (2.5 mmol), 4-chloroaniline 1.28 g (10 mmol), 40 ml of m-cresol and 4 ml of isoquinoline was heated at 50 °C for 2 h under a nitrogen atmosphere. The reaction mixture was additionally heated under nitrogen for 5 h at 130 °C, 4 h at 150 °C and 2 more hours at 200 °C. After cooling, the reaction mixture was added dropwise to acetone to give a red precipitate (N,N′-Bis (4-chlorophenyl)perylene-3,4,9,10-tetracarboxylic diimide) which was filtered, washed several times with methanol and 5% aq sodium hydroxide solution to remove isoquinoline and unreacted anhydride, then dried at 50 °C.

The prepared N,N′-Bis(4-chlorophenyl)perylene-3,4,9,10-tetracarboxylic diimide 6.11 g (10 mmol) was dissolved in 20 ml of oleum (20% SO_3) and the ensuing violet solution was heated at 145 °C for 6 h. The reaction mixture was cooled and poured into 300 ml DMF and was then added dropwise to 2,000 ml acetone, the ensuing red precipitate being filtered, washed with acetone, dried in a vacuum oven at 50 °C. Purity of the dye was confirmed by thin layer chromatography using isopropanol/acetone/ammonium water (2:2:1) as the mobile phase. The yields, ^{1}H NMR, FT-IR and Mass data of the dye are given below. Yield 65.4%;

^{1}H NMR (DMSO-d_6, ppm): 8.80 (d, 4H), 8.50 (d, 4H), 7.91 (s, 2H), 7.58 (d, 2H), 7.43 (d, 2H);

FT-IR (KBr, cm^{-1}): 1701 (C=O), 1360 (C–N), 1233, 1069 (S=O), 625 (S–O);

MALDI-TOF MS: m/z 772.05 (100%, $[M + 2H]^+$).

2.3. Thermal stabilities of the prepared dyes

The thermal stabilities of Dye 1–Dye 3 were evaluated by thermogravimetry (TGA). The prepared dyes were heated to 110 °C for 10 min to remove any residual water and solvent. Then, it was heated to 220 °C and held it for 30 min to simulate the processing thermal conditions of color filters manufacturing. The dyes were finally heated to 500 °C to determine their degradation temperature. The heating was carried out at the rate of 10 °C min^{-1} under nitrogen atmosphere [10,14].

2.4. Preparation of color inks and dye-based color filters

Three aqueous inks were prepared with different concentration (0.2 mmol, 0.22 mmol, 0.25 mmol) of synthesized dyes, distilled water (2 g) and LGM 3050 (0.68 g) as a binder based on acrylate. The binder used in this study had excellent compatibility with three dyes. Prepared dye-based inks were coated on transparent glass substrates using MIDAS System SPIN-1200D spin coater. The coating speed was kept at the rate of 300 rpm for 5 s, and then raised to 1000 rpm and kept constant for 10 s. The dye-coated color filters were prebaked at 180 °C for 30 min and subsequently baked for 1 h at 230 °C.

2.5. Geometry optimization of synthesized dyes

To analyze the difference of aggregation behaviors due to the structural difference of the dyes, dye structures were optimized through the CAChe 6.1.8 program and the intermolecular interactions that affect the aggregation were analyzed. CAChe 6.1.8 software package optimized the geometry of dye structures by using molecular mechanics MM3, conducting the iteractive energy minimizing routines with the conjugate gradient minimizer algorithm. CONFLEX conformational search procedure was used to find low-energy conformations of dye molecules. The semi-empirical method, PM5, was also examined with respect to geometry optimization, but was found to be no more satisfactory than the molecular mechanical method.

2.6. Field emission scanning electron microscopy (FE-SEM)

The aggregation size and morphology of the dyes in color filters were investigated through field emission scanning electron microscope (JEOL JAMP 9500-F). The dye aggregates were observed at an acceleration voltage of 15 kV and working distance (WD) of 8 mm, FE-SEM images of dye-based color filters were taken at the 100,000 and 150,000 magnifications.

2.7. Concentration-dependent transmittance of dye-based color filters

Transmittance spectra of the prepared dye-based color filters were measured with an HP 8452A spectrophotometer and the spectral-dependent changes were observed.

3. Results and discussion

3.1. Synthesis of dyes

Dye 1–Dye 3 were prepared through the synthetic routes illustrated in Scheme 1 and overall characterization of dye structures were carried out by ^{1}H NMR, FT-IR and Mass spectroscopy. Dye 1 is believed to exist predominantly in the hydrazone form via intramolecular hydrogen bonds. Involving the azo linkage in intramolecular hydrogen bonding, as in the case of Dye 1, would stabilize the thermally more stable hydrazone form, which could perturb the induced mesomerism and slow down the rate of dye decomposition [15]. The proton peaks involved in hydrogen bonds between N–H···O=C appear at much lower field than the normal proton peak [16] and this was confirmed by ^{1}H NMR (17.42 ppm).

Dye 2 has two N–H···O intermolecular hydrogen bonds between the NH group and the O atom. The proton peaks involved in intermolecular hydrogen bonds appear at slightly lower field than the normal proton peak of N–H [17] and were confirmed by ^{1}H NMR (11.93 ppm). Dye 1–Dye 3 contain two or three sulfonic acid groups in their structures, S=O (1233, 1069) and S–O (625) peaks were confirmed by FT-IR.

3.2. Characterization of spectral properties and thermal stabilities of dyes

UV–Visible absorption spectra of the prepared dyes in water are shown in Fig. 1 and their optical properties are collected in Table 1. Dye 2 and Dye 3 exhibited double absorption maxima (λ_{max}) at 506, 542 nm and 506, 544 nm, while Dye 1 exhibited single absorption maxima at 518 nm. All three dyes have appropriate absorption spectra for red colorants of color filters.

The thermal stabilities of Dye 1–Dye 3 through the thermogravimetric analysis (TGA) are shown in Fig. 1. The weight loss starting temperatures of the prepared dyes were 310 °C for Dye 1, 370 °C for Dye 2 and 330 °C for Dye 3. Dye 2 showed much higher thermal stability than Dye 1 and Dye 3 that could be attributed to its π–π stacked interaction, planar structure and intermolecular hydrogen bonding as explained later.

Thermal stabilities of the dyes were also investigated through measuring of their color change at 250 °C – the highest temperature in LCD manufacturing process [18,19]. As shown in Fig. 2, after heating for an hour at 250 °C absorption spectra of the three dyes were identical to those of the original dyes. Consequently, we concluded that the prepared dyes were stable at the processing thermal conditions of color filters manufacturing.

3.3. Influence of dye structure on the aggregation behaviors of dyes in color filters

3.3.1. Geometry optimization by CAChe

Fig. 3 shows the molecular geometry of Dye 1–Dye 3 optimized through CAChe program. Factors related to the intermolecular

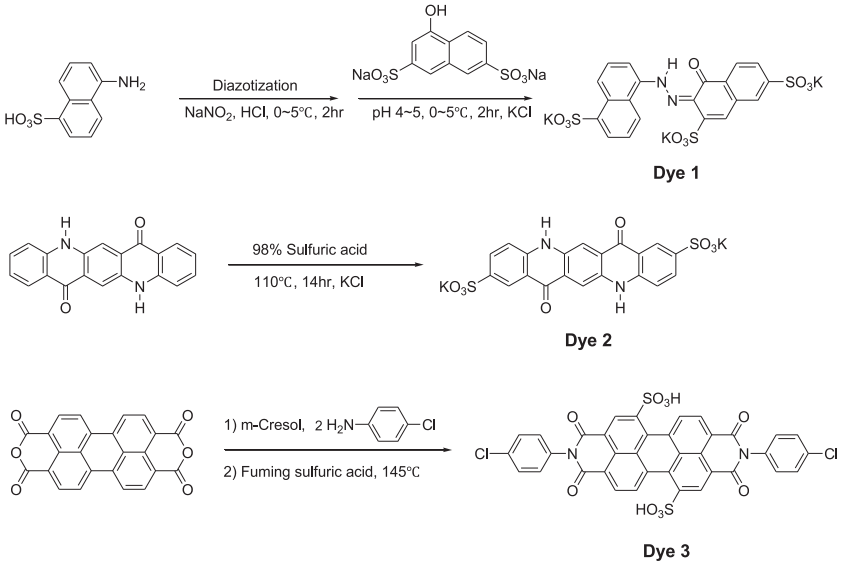

Scheme 1. Synthetic routes for the synthesis of thermally-stable red dyes.

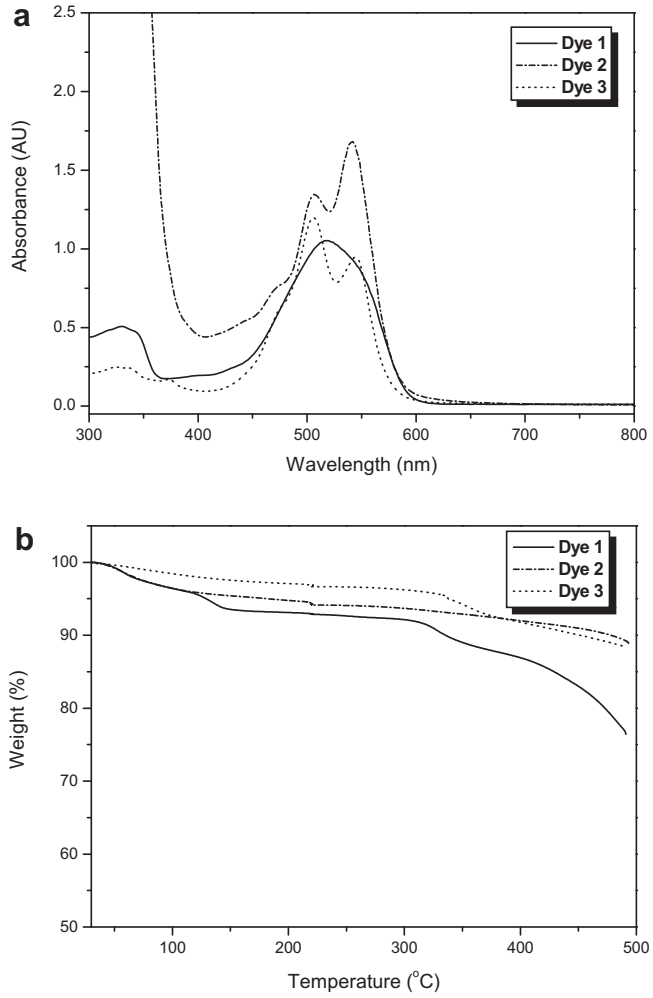

Fig. 1. Absorption spectra (a) and TGA profile (b) of the prepared dyes.

interactions that affect aggregation of dyes can be divided into three including (1) π–π stacked interaction by the aromatic ring (2) flatness of the molecular structure and (3) intermolecular hydrogen bond. There is close correlation between the factor (1) and (2) and the flatter the molecule the stronger the π–π stacked interaction [20,21].

The intermolecular π–π stacked interaction is related to the number and type of the aromatic rings included in dye molecule. The three dyes used have different numbers of aromatic rings, four for Dye 1, five for Dye 2 and nine for Dye 3. Therefore, if only the intermolecular π–π stacked interaction is considered, the degree of intermolecular interaction will be in the order of Dye 3 >> Dye 2 > Dye 1. However, from the geometrical point of view, Dye 3 has twisted perylene core, while Dye 1 and Dye 2 have excellent flatness as shown in Fig. 3.

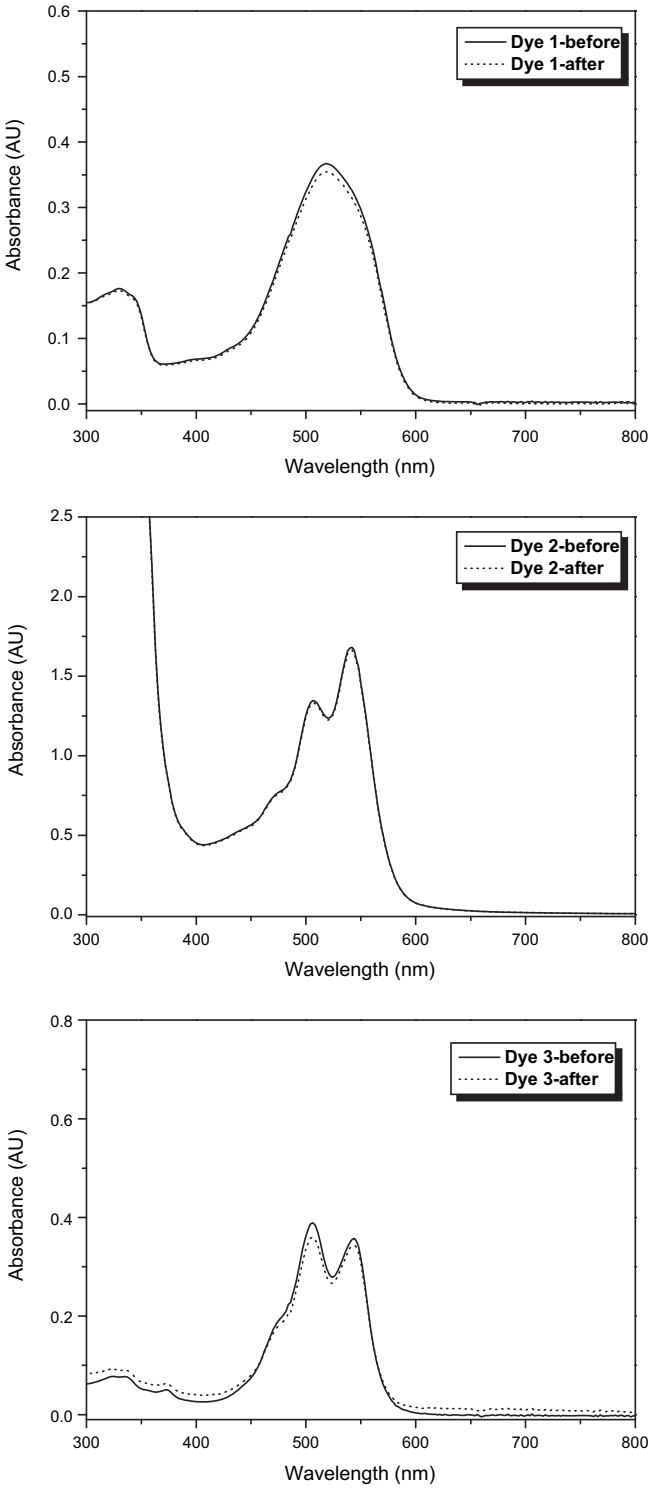

Fig. 2. Spectral changes of the prepared dyes after heating for an hour at 250 °C. (before: solid line, after: dotted line).

Table 1
Optical and thermal properties of Dye 1–Dye 3.

Dye	λ_{max}[a] (nm)	ε_{max}[a] (1 mol^{-1} cm^{-1})	Melting point (°C)
1	518	21,300	>300 (Decomp.)
2	506, 542	17,500/33,700	>300 (Decomp.)
3	506, 544	32,120/38,750	>300 (Decomp.)

λ_{max}: absorption maximum wavelength; ε_{max}: molar extinction coefficient at λ_{max}.
[a] Absorption spectra were measured in water.

Such twisted geometry of Dye 3 is caused by the introduction of bulky N-aryl groups at nitrogen atom and sulfonic acid groups at the bay position [22,23]. Therefore, the twisted structure of Dye 3 will introduce strong steric hindrance between the molecules, which results in the low degree of the intermolecular π–π stacked interaction.

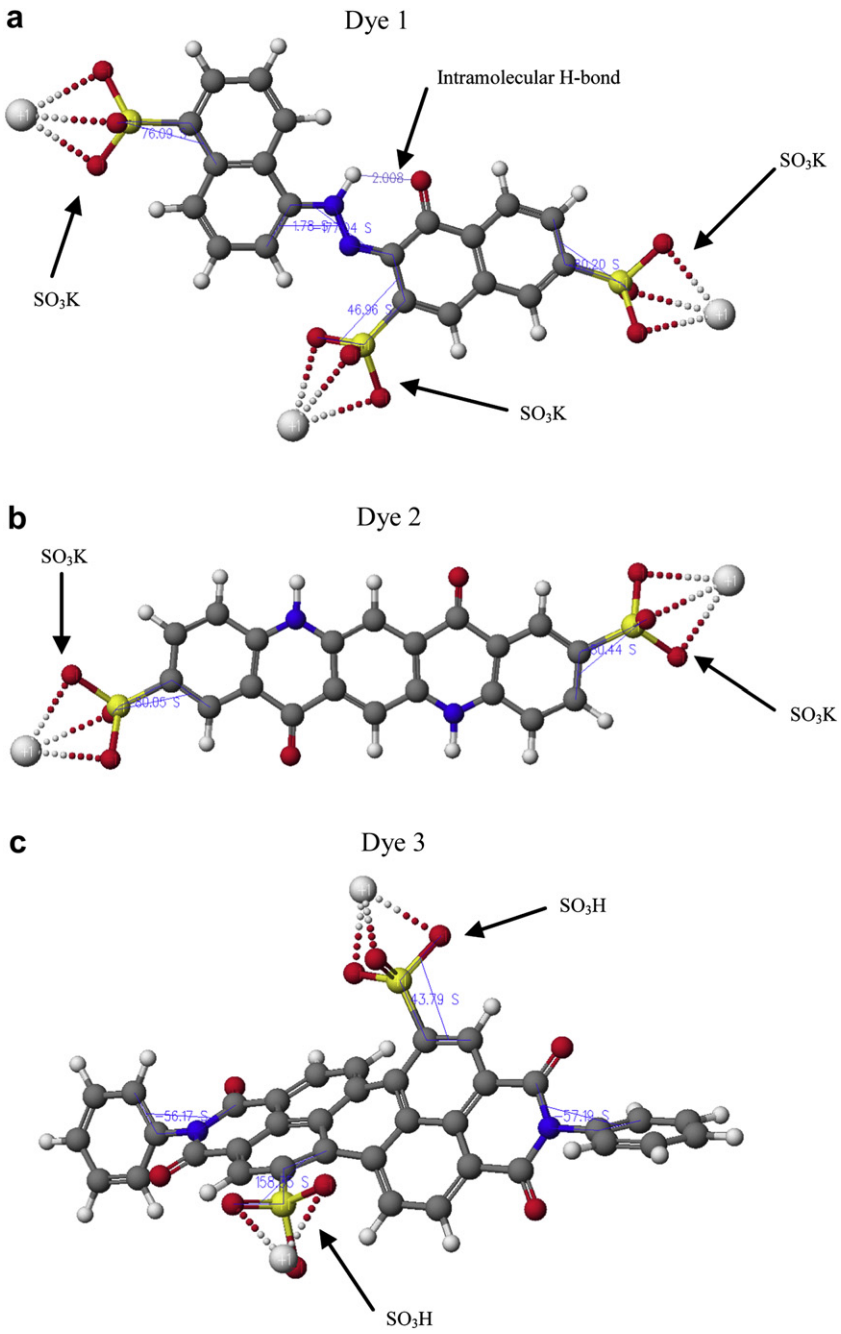

Fig. 3. Optimized molecular geometry of the prepared dyes.

On the contrary, Dye 1 and Dye 2 with less aromatic rings are too flat to decrease their intermolecular π–π stacked interaction. Especially, Dye 2 can have bifurcated N–H···O intermolecular hydrogen bonds between the NH group of one molecule and the O atom of the neighbouring one [17,24]. These interactions form a two-dimensional hydrogen-bonded network and act as an additional factor to increase the intermolecular interaction.

3.3.2. Field emission scanning electron microscopy study (FE-SEM)

The aggregate sizes of Dye 1–Dye 3 in color filters are listed in Table 2 and their FE-SEM images are shown in Fig. 4. The aggregate size decreased in the order of Dye 2 (46–100 nm) > Dye 1 (20–45 nm) > Dye 3 (15–35 nm). In order words, the aggregate size of Dye 3 that has nine aromatic rings was smaller than those of Dye 1 and Dye 2 that have four and five aromatic rings, respectively. This result corresponded with the intermolecular interaction analyzed in the optimization of the molecular structure (*3.2.1*). Although Dye 3 had more aromatic rings compared to the other dyes, steric hindrance causing twisted molecular structure

Table 2
The aggregate size and distribution of Dye 1–Dye 3 in dye-based color filters.

Dye	Range of size distribution	Average size
1	20–45 nm	35 nm
2	46–100 nm	80 nm
3	15–35 nm	25 nm

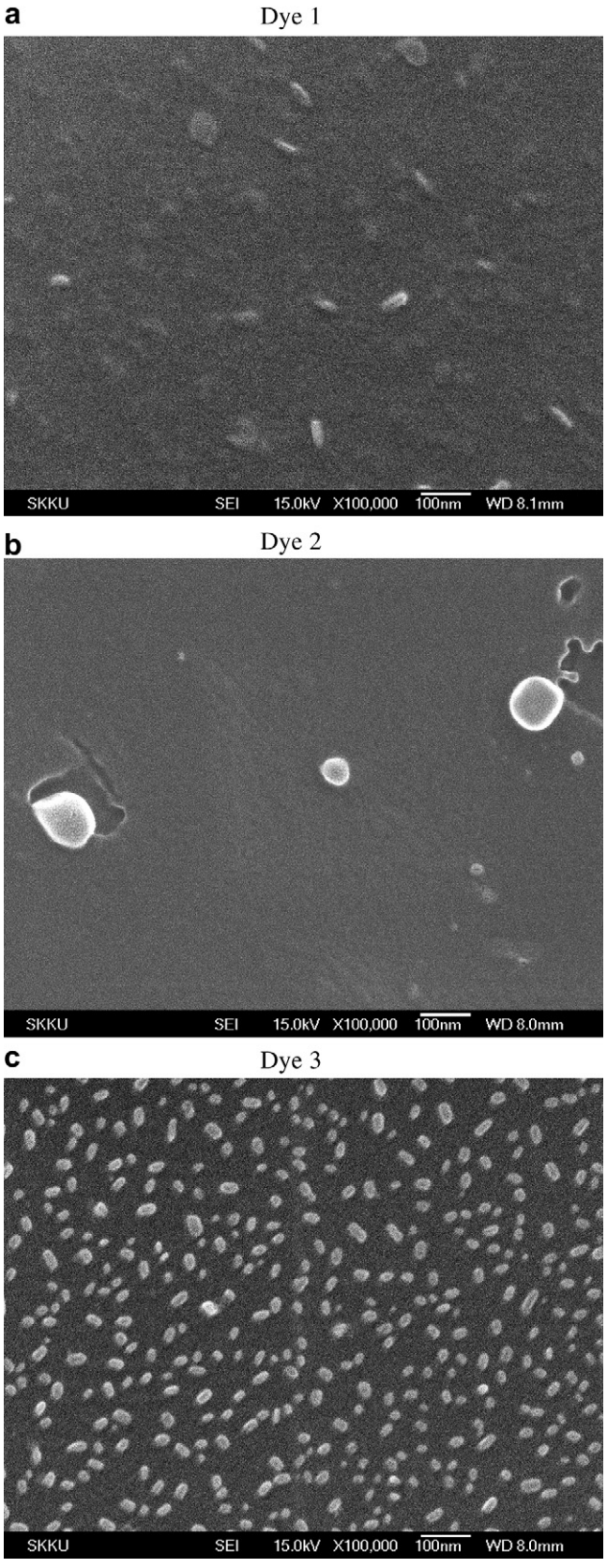

Fig. 4. FE-SEM images of dye aggregates in 0.2 mmol dye-based color filters.

decreased the intermolecular π-π stacked interaction between the molecules, and resulted in the relatively smaller aggregations. Even though Dye 1 and Dye 2 had less aromatic rings, they formed larger dye aggregates owing to their planar structure. Especially, Dye 2 could form four intermolecular hydrogen bonds with its neighbouring molecules and its aggregate size reached almost 100 nm as shown in the FE-SEM results (Fig. 4).

Fig. 5 shows the images of dye aggregates in color filters at higher dye concentration of 0.25 mmol. The sizes of dye aggregates for Dye 1 and Dye 3 increased considerably as the concentration of dye in color filters increased. Whereas dye concentration in color filters only increased by 1.25 times, the size of dye aggregates rapidly increased by 1.7 times and 1.6 times for Dye 1 and Dye 3. In case of Dye 2, the size of dye aggregate was so large that we could not report the image of aggregates in this paper.

3.3.3. The influence of dye aggregation on the spectral properties of the color filters

Fig. 6 shows the transmittance spectra of the dye-based color filters. Dye 1 and Dye 3 showed very small change of the transmittance spectrum for each concentration within the long wavelength region (600 nm–700 nm). However, the spectra became

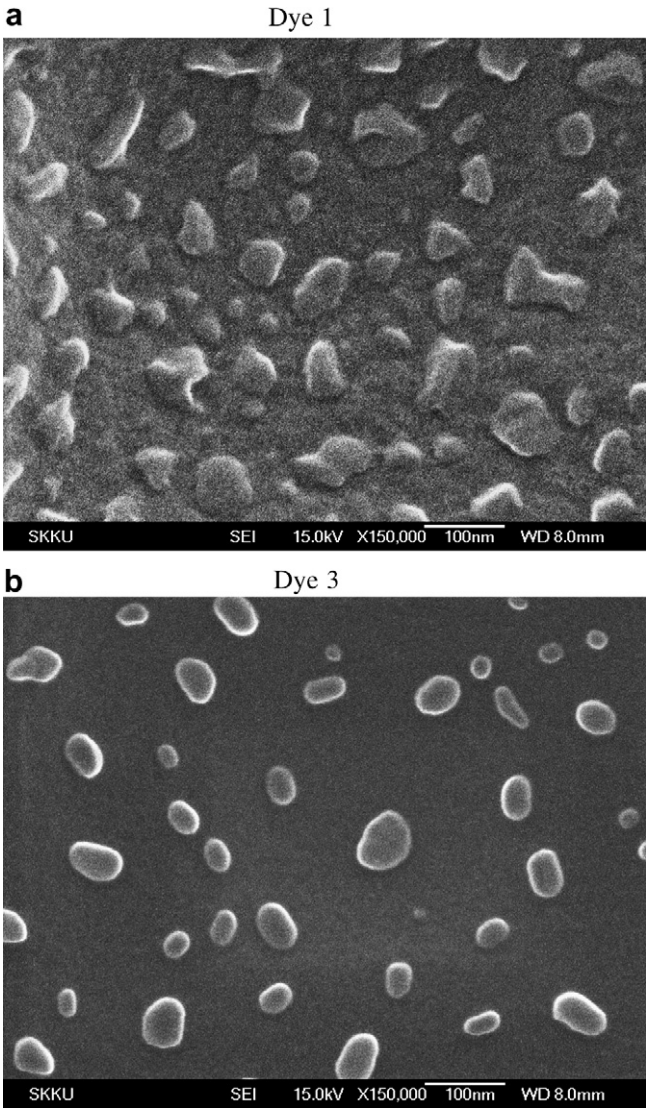

Fig. 5. FE-SEM images of dye aggregates in 0.25 mmol dye-based color filters.

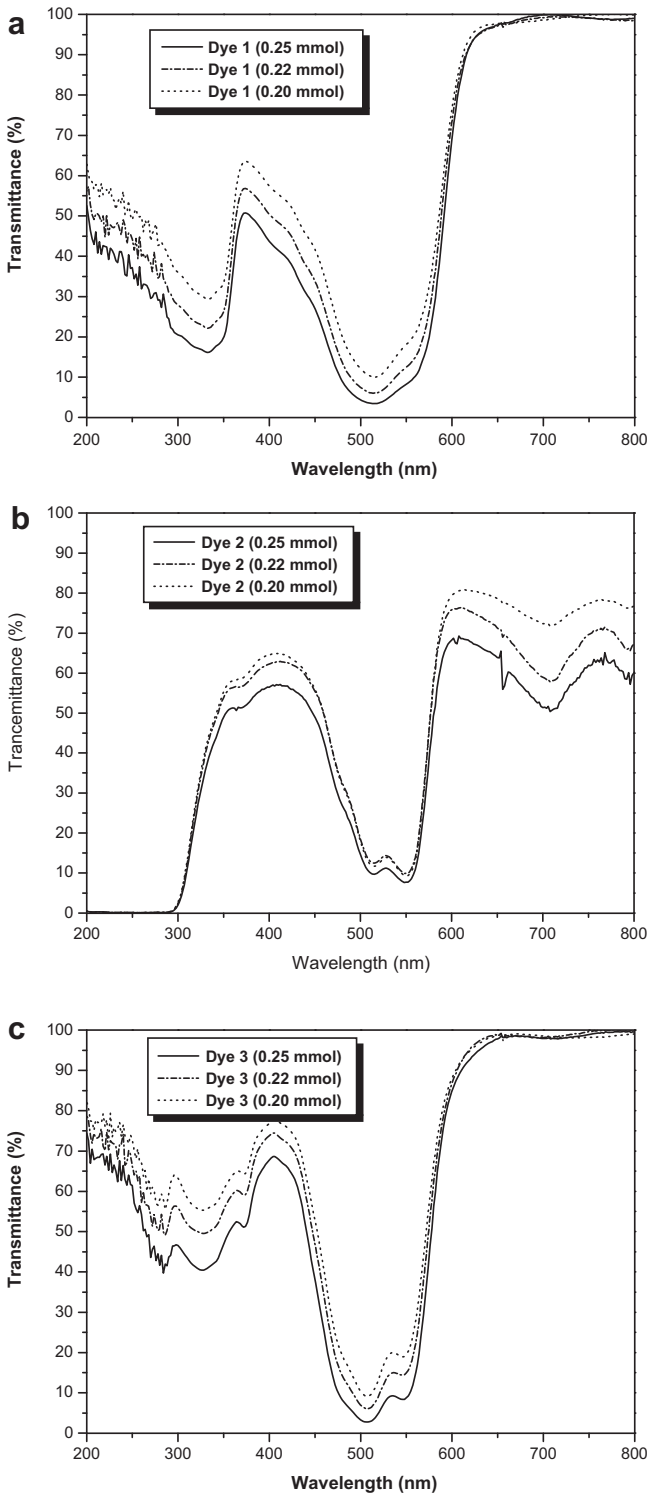

Fig. 6. Concentration-dependent transmittance spectra of dye-based color filters. (a) Dye 1 with concentrations of 0.25, 0.22, 0.20 mmol (b) Dye 2 with concentrations of 0.25, 0.22, 0.20 mmol (c) Dye 3 with concentrations of 0.25, 0.22, 0.20 mmol.

broader across the whole wavelength as the concentration increased. In case of Dye 2, in particular, formation of a new absorption band was observed within the longer wavelength region near 700 nm as the concentration of dye increased. This is considered due to the higher aggregation of Dye 2 as shown in the FE-SEM results (Fig. 4). It has been known that dye aggregation influences the ground state of dyes and creates additional absorption band [25–27]. As a result, new absorption band can appear within the longer wavelength range which could decrease the transmittance of red color filters. In case of Dye 1 and Dye 3, new absorption band within the longer wavelength was very small compared to that of Dye 2 and this was believed to be due to less aggregation of them.

Table 3
The color coordinate values corresponding to CIE 1931 chromaticity diagram of dye-based color filters.

Color filters	Concentration	*x*	*y*	Y
Dye 1	0.20 mmol	0.435	0.303	36.52
	0.22 mmol	0.467	0.304	30.98
	0.25 mmol	0.503	0.305	26.05
Dye 2	0.20 mmol	0.421	0.297	28.23
	0.22 mmol	0.453	0.298	25.48
	0.25 mmol	0.486	0.299	20.39
Dye 3	0.20 mmol	0.397	0.286	48.64
	0.22 mmol	0.407	0.284	44.76
	0.25 mmol	0.433	0.279	38.29

Table 3 illustrates the measured color coordinate values of (x, y) and the brightness of Y in the CIE 1931 chromatic diagram for different concentration of dye-based color filters. Color coordinate values of x tend to be wider with an increase in concentration of red dyes.

4. Conclusion

Three thermally-stable red dyes were synthesized and dye-based color filters were manufactured with them. The relationship between dye aggregation and spectral characteristics of the prepared color filters was analyzed. The aggregate sizes of prepared dyes were proportional to their strength of intermolecular interaction involving $\pi-\pi$ stacked interaction, hydrogen bonding and molecular geometry. As the aggregate sizes of dyes increased, the transmittance of color filters decreased.

To improve the thermal stability of dyes for LCDs color filters, molecular structures of the dyes should be designed to increase their intermolecular interactions. However, stronger intermolecular interaction could lead to higher dye aggregation, resulting in significantly decreased transmittance of color filters. Therefore, the aggregation of dye molecule should be carefully controlled so that the color filters could have good transmittance while its thermal resistance is not impaired.

Acknowledgements

This work was supported by a grant from the Fundamental R&D Program for Core Technology of Materials funded by the Ministry of Knowledge Economy, Republic of Korea.

References

[1] Sabnis RW. Color filter technology for liquid crystal displays. Displays 1999;20:119–29.
[2] Tsuda K. Color filters for LCDs. Displays 1993;14:115–24.
[3] Takanori K, Yuki N, Yuko N, Hidemasa Y, Kang WB, Pawlowski PG. Polymer optimization of pigmented photoresists for color filter production. Jpn J Appl Phys 1998;37:1010–6.
[4] Na DY, Jung IB, Nam SY, Yoo CW, Choi YJ. The rheological behavior and dispersion properties of millbase for LCD colorfilters. J Korean Inst Electr Electron Mater Eng 2007;20:450–5.
[5] Calvert P. Inkjet printing for materials and devices. Chem Mater 2001;13:3299–305.
[6] Chang CJ, Chang SJ, Shin KC, Pan FL. Improving mechanical properties and chemical resistance of ink-jet printer color filter by using diblock polymeric dispersants. J Polym Sci B Polym Phys 2005;43:3337–53.

[7] Koo HS, Chen M, Pan PC, Chou LT, Wu FM, Chang SJ, et al. Fabrication and chromatic characteristics of the greenish LCD colour-filter layer with nano-particle ink using inkjet printing technique. Displays 2006;27:124–9.
[8] Koo HS, Chen M, Pan PC. LCD-based color filter films fabricated by pigment-based colorant photo resist inks and printing technology. Thin Solid Films 2006;515:896–901.
[9] Sugiura T. Dyed color filters for liquid-crystal displays. J Soc Inf Disp 1993;1:177–80.
[10] Kim YD, Kim JP, Kwon OS, Cho IH. The synthesis and application of thermally stable dyes for ink-jet printed LCD color filters. Dyes Pigm 2009;81:45–52.
[11] Song DH, Yoo HY, Kim JP. Synthesis of stilbene-based azo dyes and application for dichroic materials in poly(vinyl alcohol) polarizing films. Dyes Pigm 2007;75:727–31.
[12] Smith JA, West RM, Allen M. Acridones and quinacridones:Novel fluorophores for fluorescence lifetime studies. J Fluoresc 2004;14:151–71.
[13] Bodapati JB, Icil H. Highly soluble perylene diimide and oligomeric diimide dyes combining perylene and hexa(ethylene glycol) units: synthesis, characterization, optical and electrochemical properties. Dyes Pigm 2008;79:224–35.
[14] Guerrero DJ, DiMenna B, Flaim T, Mercado R, Sun S. Dyed red, green, and blue photoresist for manufacture of high-resolution color filter arrays for image sensors. Proc Soc Photo Opt Instrum Eng 2003;5017:298–306.
[15] Moien B, Ezzeldine HM, Ibrahim M, Ismail M. Thermal decomposion stages of the azo linkages in novel azo phosphorus compounds; A correlative DTA study. Thermochimica Acta 1992;198:21–31.
[16] Skrabal P, Zollinger H. Mechanism of azo coupling reactions: part XXXV. pH-dependence and ortho/para ratio in coupling reactions of amino-hydroxynaphthalenesulfonic acids. Dyes Pigm 1988;9:201–7.
[17] Mizuguchi J, Senju T. Solution and solid spectra of quinacridone derivatives as viewed from the intermolecular hydrogen bond. J Phys Chem B 2006;110:19154–61.
[18] Das S, Basu R, Minch M, Nandy P. Heat-induced structural changes in merocyanine dyes: X-ray and thermal studies. Dyes Pigm 1995;29: 191–201.
[19] Chunlong Z, Nianchun M, Liyun L. An investigation of the thermal stability of some yellow and red azo pigments. Dyes Pigm 1993;23:13–23.
[20] Kim JH, Masaru M, Fukunishi K. Three dimensional molecular stacking and functionalities of aminonaphthoquinine by intermolecular hydrogen bondings and interlayer π-π interactions. Dyes Pigm 1998;40:53–7.
[21] Thetford D, Cherryman J, Chorlton AP, Docherty R. Theoretical molecular modeling calculations on the solid state structure of some organic pigments. Dyes Pigm 2004;63:259–76.
[22] Würthner F, Thalacker C, Diele S, Tschierske C. Fluorescent J-type aggregates and thermotropic columnar mesophases of perylene bisimide dyes. Chem Eur J 2001;7:2245–52.
[23] Chao CC, Leung M. Photophysical and electrochemical properties of 1,7-diaryl-substituted perylene diimides. J Org Chem 2005;70:4323–31.
[24] Keller U, Müllen K, De Feyter S, De Schryver FC. Hydrogen-bonding and phase-forming behavior of a soluble quinacridone. Adv Mater 1996;8: 490–3.
[25] Kobayashi T. J-Aggregates. Singapore: World Scientific; 1996.
[26] Mishra A, Behera RK, Behera PK, Mishra BK, Behera GB. Cyanines during the 1990s: a review. Chem Rev 2000;100:1973–2011.
[27] Eisfeld A, Briggs JS. The J- and H-bands of organic dye aggregates. Chem Phys 2006;324:376–84.